Available online at www.sciencedirect.com
ScienceDirect
Materials Research Bulletin 42 (2007) 1040–1050
Materials Research Bulletin
www.elsevier.com/locate/matresbu

Influence of Mg-substitution on the physicochemical properties of calcium phosphate powders

J. Marchi [a,b], A.C.S. Dantas [a], P. Greil [a], J.C. Bressiani [b], A.H.A. Bressiani [b], F.A. Müller [a,*]

[a] *University of Erlangen-Nuernberg, Department of Materials Science-Biomaterials, Henkestr. 91, D-91052 Erlangen, Germany*
[b] *Institute of Energetic and Nuclear Research (IPEN), Centre of Science and Materials Technology, Department of Ceramics, Av. Prof. Lineu Prestes, 2242, 05508-000 São Paulo, SP, Brazil*

Received 21 February 2006; received in revised form 13 September 2006; accepted 20 September 2006
Available online 7 November 2006

Abstract

Tricalcium phosphate based ceramics (TCP) are bioresorbable and thereby considered to be promising bone replacement materials. The differences in crystal structure between α and β-TCP phases gives rise for different dissolution rates *in vitro* and *in vivo*, which may alter the bioresorbable behavior of TCP ceramics. It is suggested that the addition of magnesium ions, which are also present in biological tissues, stabilizes β-phase to higher temperatures and thus enables the sintering of β-TCP at elevated temperatures compared to Mg free TCP.

In this paper, Mg-substituted TCP, with the general formula $(Ca_{1-x}Mg_x)_3(PO_4)_2$ and $0.01 \leq x \leq 0.045$, were produced by wet chemical synthesis from $Ca(OH)_2$, H_3PO_4 and MgO, after calcinations at three different temperatures between 750 and 1050 °C. The influence of different amounts of Mg substitution on the physical properties, microstructure, and sintering behavior of calcium phosphate powders was evaluated. Thermal analytical techniques, together with X-ray diffraction analysis, were successfully combined in order to characterize the occurring phase transformations during annealing of the powders. The results show that the addition of small amounts of Mg (up to 1.5 mol%) are adequate to postpone the β–α TCP phase transformation to 1330 °C and to accelerate the densification process during sintering of β-TCP ceramics.

Keywords: A. Ceramics; B. Chemical synthesis; C. X-ray diffraction; D. Thermodynamic properties

1. Introduction

Calcium phosphate based ceramics are promising synthetic materials used as an alternative to autograph and allograph implants in bone replacement surgery [1,2]. The similarity to the chemical composition of bone leads to a high bone bonding ability of these inorganic materials. Among calcium phosphate ceramics, tricalcium phosphate ($Ca_3(PO_4)_2$, TCP), a resorbable material, and hydroxyapatite ($Ca_{10}(PO_4)_6(OH)_2$, HAp), a bioactive ceramic, that induces bone formation on its surface, received particular attention [2,3]. Other phases, such as dicalcium phosphate ($Ca_2P_2O_7$, DCP) and tetracalcium phosphate ($Ca_4P_2O_9$, TetTCP), have also been studied for application in medical fields [3].

* Corresponding author. Tel.: +49 9131 8525543; fax: +49 9131 8525545.
E-mail address: Frank.Mueller@ww.uni-erlangen.de (F.A. Müller).

0025-5408/$ – see front matter © 2006 Elsevier Ltd. All rights reserved.
doi:10.1016/j.materresbull.2006.09.015

TCP exists in four crystalline structures [4]. The β-TCP phase with a theoretical density of 3.07 g/cm^3 is stable up to 1125 °C. Heating above this temperature, β- to α-phase transformation gives rise for a 7.24% volume expansion. α-TCP phase with a theoretical density of 2.86 g/cm^3 is stable up to 1430 °C. The other crystalline structures of tricalcium phosphate, α', which is stable above 1430 °C and γ, a high pressure form, are difficult to obtain due to their metastability [5].

The high reactivity, and, consequently, high rate of dissolution of α-TCP *in vitro* and *in vivo* limits its biomedical application [6]. On the other hand, the lower dissolution rate of β-TCP together with the suitable characteristics of chemical stability and mechanical strength fulfill the requirements for resorbable bone replacement materials [7].

TCP ceramics can be prepared through solid state reaction and by wet chemical synthesis, both from various precursors or reactants [8,9]. Studies of ion substitutions into calcium phosphate phases are of great importance due to the fact that major components of biological tissues, such as bone, teeth and some invertebrate skeletons are composed of an apatitic mineral phase containing a variety of other elements [10,11]. Magnesium is considered the most important ion used in calcium substitution, leading to a change in the biological and chemical behavior of these materials [12]. It was observed that the amount of Mg^{2+} incorporated into calcified tissues associated with the apatitic phase decreases with stronger calcification, leading to changes of the bone matrix that determines the bone fragility [9]. Thus, if Mg^{2+} ions were incorporated into calcium phosphate ceramics, it is expected that the *in vivo* behavior of this synthetic materials is more similar to bone mineral, as compared to Mg free synthetic materials [13]. Moreover, considering tricalcium phosphate, it is well known that the low temperature β-TCP phase is stabilized by solid solution formation through the incorporation of metal ions on the Ca(V) site of the β-TCP lattice, leading to higher transformation temperature into α-TCP [14]. Simultaneously, the presence of Mg ions in the TCP lattice inhibits the grain growth during sintering [15].

Magnesium ions can be introduced in the calcium phosphate powders by mixing a Mg oxide (or hydroxide) with crystalline TCP powders or by Mg addition into reagents during TCP powder synthesis [16–20]. Few researches are involved in systematical studies of calcium phosphate ceramics doped with magnesium [6,9,21–23]. However, in most of the earlier studies, MgO was incorporated into HAp or TCP powders after synthesis without a substituting character. In this paper, Mg was added during wet chemical synthesis of tricalcium phosphate powders. The aim of this work was to investigate the effect of the Mg substitution for Ca on the particle size distribution, morphology and specific surface area of the resulting calcium phosphate powders.

2. Materials and methods

2.1. Preparation

Calcium deficient hydroxyapatite ($Ca_{10-x}(HPO_4)_x(PO_4)_{6-x}(OH)_{2-x}$, CDHA) with various Mg content was wet chemically synthesized from calcium hydroxide ($Ca(OH)_2$, p.a., Merck), magnesium oxide (MgO, p.a., Merck) and orthophosphoric acid (H_3PO_4, p.a., 85%, Merck). 0.1 M $Ca(OH)_2$ solution was mixed with MgO powder under magnetic stirring for 1 h, in order to dissolve the powders into distilled water. An aqueous solution of 0.3 M $H_3(PO_4)$ was added under rigorous stirring to obtain a clear solution.

Precipitation occurred from the precursors solutions, following the chemical reaction

$$(9 - 9x)Ca(OH)_2 + 6H_3PO_4 + 9xMgO \rightarrow (Ca_{1-x}Mg_x)_9(HPO_4)(PO_4)_5OH + (17 - 9x)H_2O + 4.5xO_2 \quad (1)$$

with $0.01 \leq x \leq 0.045$. The suspensions were aged for 24 h, filtered, washed with double distilled water and freeze dried for 3 h at −30 °C and 37 Pa (Christ, LMC2, Delta 2-24, Germany).

The powders were calcinated in an electrically heated furnace (Nabertherm, HT16716, Germany) in air at a temperature of 750, 900 and 1050 °C, respectively, in order to transform the CDHA powders into Mg-doped TCP

$$(Ca_{1-x}Mg_x)_9(HPO_4)(PO_4)_5OH \rightarrow 3(Ca_{1-x}Mg_x)_3(PO_4)_2 + H_2O \quad (2)$$

Heating and cooling rates of 10 °C/min and a dwell time of 3 h were applied.

2.2. Characterization

X-ray diffraction analyses (XRD, Siemens, D 500 equipped with a Anton Paar HTK 10 chamber, Germany) were performed in the 2θ range between 20° and 38° at room temperature, from 500 to 1350 °C within 50 °C intervals and again after cooling to room temperature. The diffraction patterns were compared with JCPDS database 46-905 (CDHA), 9-169 (β-TCP) and 29-395 (α-TCP). The length of coherent domains $r_{(2\,0\,10)}$ in TCP crystallites was calculated using the line broadening of the (2 0 10) peak, according to Scherrer's equation

$$r_{(2\,0\,10)} = \frac{K\lambda}{\mathrm{FWHM}\cos\theta} \tag{3}$$

with the shape factor K (0.9), the X-ray $Cu_{\alpha I}$ wavelength λ (1.5418 Å), FWHM (full width at half maximum), and the diffraction angle 2θ (31.0°).

The calcium to phosphorous molar ratio, as well as the exact amount of Mg in the precipitated and calcinated powders, were obtained by inductive coupled plasma-optical emission spectrometry analysis (ICP-OES, Spectro Analytical Instruments, Germany). Duplicate measurements were performed using 50 mg calcium phosphate powders dissolved into 20 ml (HNO_3:H_2O) solution.

The Brunnauer Emmet Teller method (BET) was used to determine the specific surface area of the powders, prior and after calcination (Micromeritics, ASAP 2000, USA). Powders were heated to 350 °C before analysis, to remove all the adsorbed water present in the apatite structure.

The particle size distribution was evaluated by a laser scanning technique (Malvern Instruments, Mastersizer APA 2000, England). To reduce the particles agglomeration tendency, all powders were ultrasonically treated in tetra sodium pyrophosphate ($Na_4P_2O_7{\cdot}10H_2O$, Merck) and double distilled water for 10 min. The powder morphology was examined by scanning electron microscopy (SEM) of gold sputtered samples (FEI, Quanta 200, The Netherlands). Differential thermal analyses (DTA, Netzsch, STA 400, Germany) were performed in dynamic air flow. A heating rate of 10 °C/min and a dwell time of 1 h at 1400 °C were utilized. Sintering behavior was investigated by dilatometric experiments (Netzsch, E7/402, Germany) in an alumina tube using the same temperature conditions as for the thermal analysis. Pellets of 6 mm diameter were prepared from dried powders by uniaxial pressing with a pressure of 20 MPa. Species had a typical green density of 52% theoretical density.

3. Results and discussion

3.1. Powder characteristics

ICP measurements (Table 1) indicate that powders prepared with calcium hydroxide and orthophosphoric acid without magnesium oxide addition during synthesis contain 0.22 wt.% Mg (0.9 mol% Mg). This Mg content results from magnesium impurities in commercial calcium hydroxide. Consequently, the magnesium oxide amount additionally added during synthesis was calculated in order to obtain powders that contain 1, 1.5 and 4.5 mol% Mg (herein called 1, 1.5 and 4.5 Mg, respectively). In all powders, the (Ca + Mg)/P molar ratio was adjusted to ~1.45. Thus, the $Ca_2P_2O_7$ phase is also expected to be present in all powders.

Fig. 1 shows the diffraction patterns of 1 and 4.5 Mg powders after annealing to different temperatures. The position of the peaks are shifted towards lower 2θ values as the temperature is increased due to the thermal expansion. CDHA is obtained after precipitation at room temperature and keeps its stability up to temperatures as high as 700 °C. The transformation of CDHA into β-TCP according to the reaction described in Eq. (2) occurs at temperatures

Table 1
Chemical composition of as prepared calcium phosphate powders

Powders	Weight (%)			Mg (mol%)	Mg extra addition (mol%)	(Ca + Mg)/P molar ratio
	Mg	P	Ca			
1 Mg	0.22	20.41	37.70	0.905	–	1.44
1.5 Mg	0.33	20.35	37.83	1.358	0.5	1.45
4.5 Mg	1.05	20.64	36.73	4.32	3.5	1.44

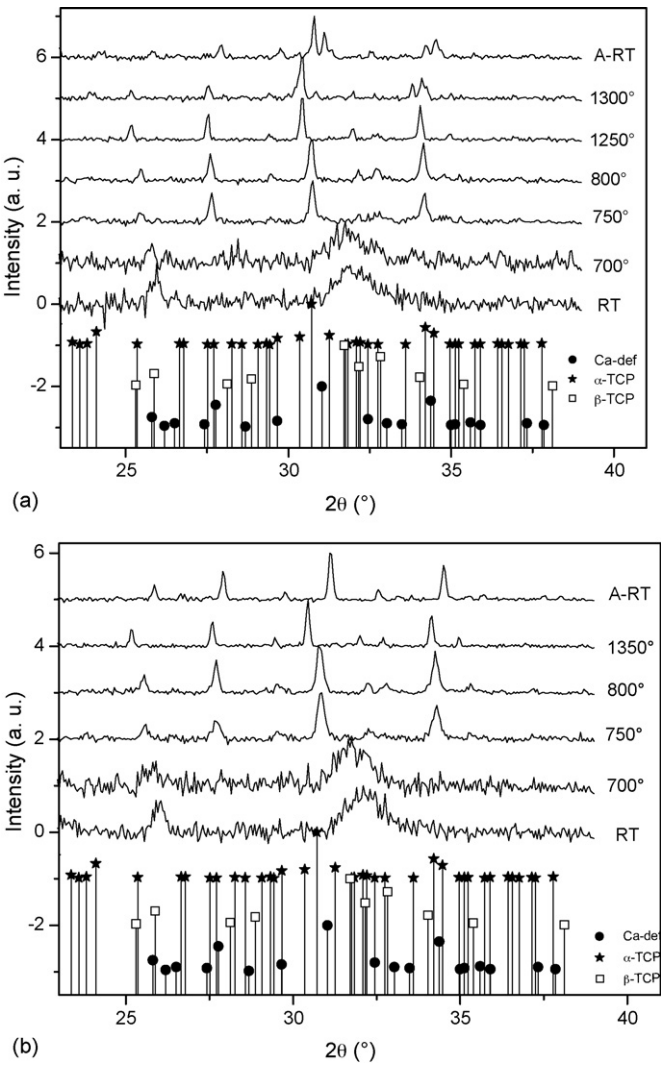

Fig. 1. X-ray diffraction pattern as a function of temperature of calcium phosphate powders: (a) 1 Mg powder and (b) 4.5 Mg powder. RT: room temperature analysis; A-RT: analysis at room temperature after annealing to 1350 °C.

between 700 and 750 °C. Above 1250 °C the β-TCP phase in 1 Mg specimen starts to transform into α-TCP, whereas 4.5 Mg specimen shows no phase transformations up to 1350 °C. The diffraction patterns obtained from 1 Mg powders annealed to 1350 °C and subsequently cooled down to room temperature still indicate the presence of α-TCP. Using Scherrer's equation coherent domain sizes of 41 and 27 nm were found for 1 and 4.5 Mg samples calcinated at 750 °C, respectively. Increasing the calcinations temperature to 1250 °C increases domain sizes to 69 and 59 nm for 1 and 4.5 Mg samples, respectively.

Fig. 2 shows the expanded X-ray diffraction pattern of 1 and 4.5 Mg samples after annealing to 750 and 1200 °C, respectively. X-ray diffraction planes corresponding to (*h k l*) = (2 1 4), (0 2 10) and (2 1 8) β-TCP peaks are marked for the 1 Mg peak position. It can be observed that incorporation of magnesium into the TCP lattice involves a shift of diffraction peaks to higher 2θ values, due to a reduction of lattice parameters caused by the smaller ionic radius of Mg^{2+} compared to Ca^{2+}. These results are in good agreement with the comparison between peaks positions from the JCPDS cards of β-TCP (09-0169) and β-TCP with 4.67 mol% magnesium substitution ($(Ca_{0.9533}Mg_{0.0467})_3(PO_4)_2$, 70-0681).

The results of specific surface area measurements are presented in Fig. 3. With increasing calcination temperature the specific surface area is significantly reduced due to diffusion controlled smoothening of the particles surfaces at

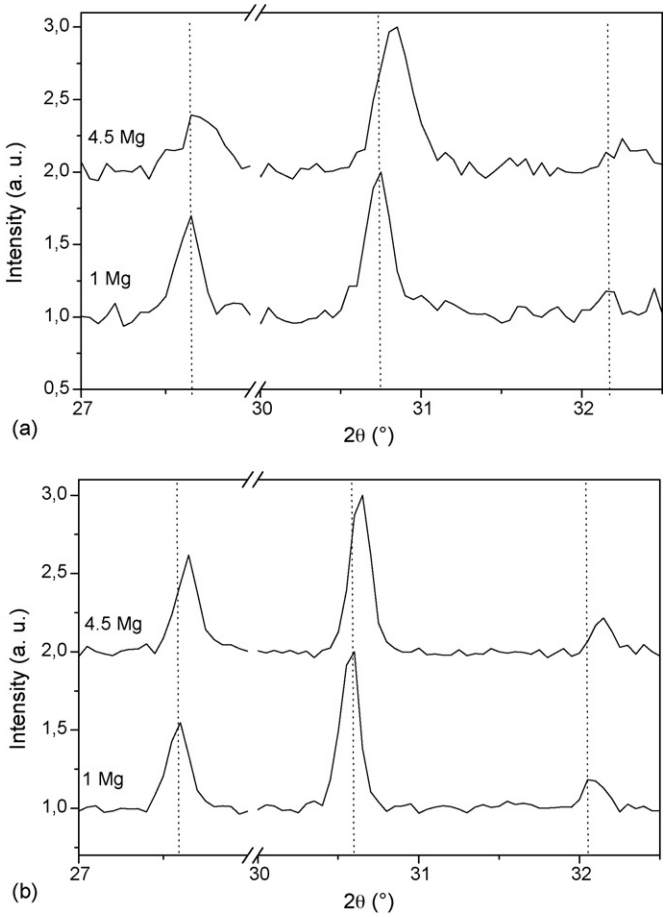

Fig. 2. Expanded X-ray diffraction pattern comparing the (2 1 4), (0 2 10) and (2 1 8) β-TCP peak position of 1 Mg powders and 4.5 powders, after calcinations for 3 h at (a) 750 °C and (b) 1050 °C.

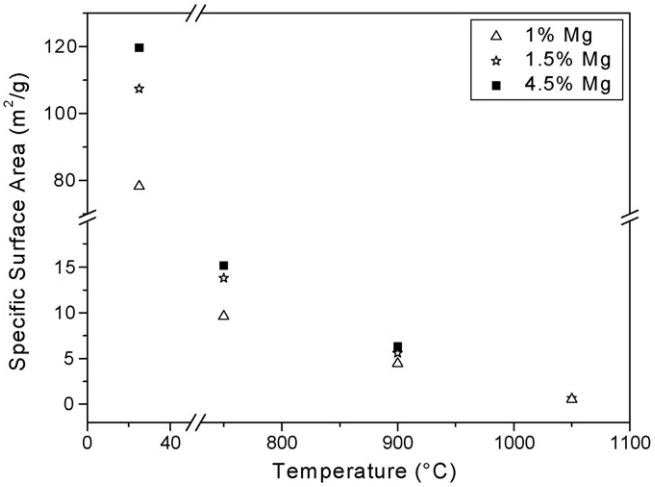

Fig. 3. Specific surface area of calcium phosphate powders with different amount of Mg substitution as synthesized and after calcination at 750 °C, 900 °C and 1050 °C for 3 h.

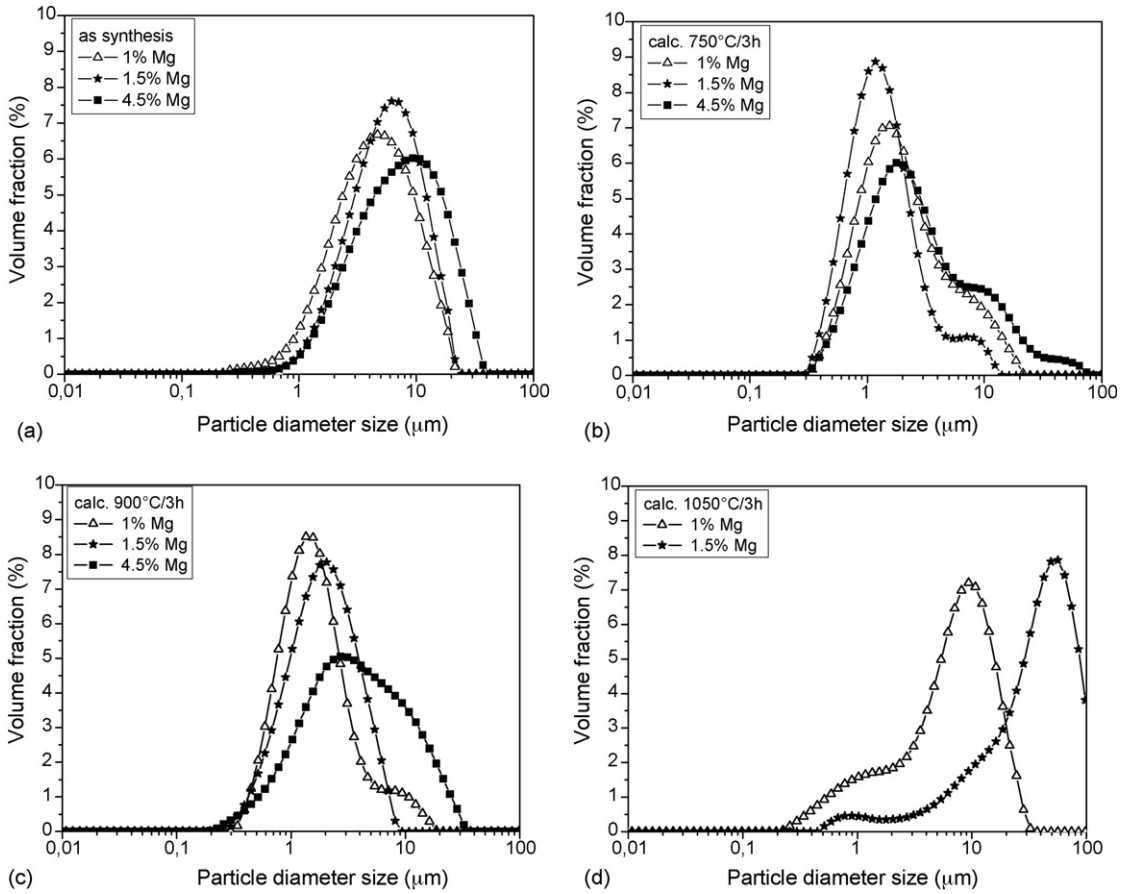

Fig. 4. Particle size distribution of calcium phosphate powders with Mg substitution: (a) as synthesized; (b) after calcination at 750 °C for 3 h; (c) after calcinations at 900 °C for 3 h; (d) after calcinations at 1050 °C for 3 h.

elevated temperatures. Mg incorporation leads to an increase of the specific surface area of approximately 50% for precipitated 4.5 Mg powders compared to 1 Mg powders. Considering the same calcination temperature, Mg incorporation increases the specific surface area of powders and, consequently, leads to a higher powder reactivity.

Results of particle size distribution reveal two different effects (Fig. 4). During annealing the particle size of as synthesized powders first decreases to a minimum at a calcination temperature around 750 °C due to a breaking effect of agglomerated precipitates, that is initiated by the loss of water during the transformation of CDHA to β-TCP (Eq. (2)). At temperatures above the transformation temperature the particle size increases by grain coarsening due to initial sintering effects. Particles start to agglomerate. As can be seen in Table 2, the particle size in general increases with increasing magnesium content. All particle size distributions of CDHA powders are uni-modal for as synthesized powders, independent of the magnesium content (Fig. 4a). However, calcination at 750 °C for 3 h alters the distribution to a bimodal behavior, indicating that the particles start sintering after the CDHA to TCP transformation is completed.

The particle size distribution observed for powders calcinated at 900 °C for 3 h (Fig. 4c) indicates that powders with lower Mg amounts (represented as △) are still in the initial stage of sintering. On the other hand, powders with higher Mg content (represented as ■) show a broadening of the particle size distribution, indicating that these powders started the sintering process at lower temperatures. Thus, the presence of Mg might be responsible for the acceleration of the sintering process.

Powders calcinated at 1050 °C for 3 h are already in the intermediate stage of sintering, as indicated by the growth of the shoulder in the bimodal particle size distribution to form a peak with the highest intensity (Fig. 4d and Table 2). The particle size distribution analysis of the 4.5 Mg powders calcinated at this temperature was not possible due to the

Table 2
d_{50} values (μm) of calcium phosphate powders with different amount of Mg substitution (mol%)

	1 Mg	1.5 Mg	4.5 Mg
As synthesized	4.4	5.6	7.4
Calcined at 750 °C/3 h	1.8	1.3	2.4
Calcined at 900 °C/3 h	1.5	1.9	3.5
Calcined at 1050 °C/3 h	7.1	39.2	–

sintered character of this powder. Moreover, there is a great increase in the d_{50} values for these powders (Table 2), due to neck growth and loss of porosity during the intermediate stage of sintering.

Considering the same calcination temperature, there is, in general, an increase in average particle size d_{50} with an increasing amount of magnesium substituting calcium in the TCP lattice (Fig. 4 and Table 2). This behavior is accentuated in powders calcinated at 1050 °C for 3 h (Fig. 4d).

3.2. Microstructure and phase transformation

Fig. 5 illustrates the particle morphology as a function of different calcination temperatures for 1.5 Mg powders. First, a decrease in agglomeration size to a minimum value compared to as synthesized powder (Table 2) occurs during calcinations at 750 °C. With increasing temperature, the particle size increases due to sintering of the powders. Powders calcinated at 900 °C show the formation of necks between single particles (Fig. 5b), which are characteristic for the initial stage of sintering.

Moreover, it can be noticed that powders calcinated at 1050 °C for 3 h (Fig. 5c) are already sintered. Residual pores are homogeneously distributed in the calcium phosphate matrix. The powder morphology is similar considering the other compositions with different amounts of magnesium incorporated into TCP lattice calcined at same temperature. Thus, these observations confirm the results of specific surface area and particle size distribution measurements. The higher specific surface area values of uncalcinated powders can be related to a higher roughness in the powder morphology. SEM results indicate that the laser scanning technique measures the agglomerate size of calcium phosphate powders, instead of particle size.

The influence of magnesium substitution into the lattice on the transformation was determined by differential thermal analysis (Fig. 6). An exothermic process related to the loss of water is observed in all powders up to 400 °C. The CDHA → TCP transformation is characterized by an exothermic reaction immediately followed by an endothermic process corresponding to dehydroxylation of CDHA and, consequently, β-TCP phase formation. This transformation occurs at temperatures between 700 and 800 °C for all powders, although the presence of magnesium substituted in the calcium phosphate lattice alters the transformation from CDHA to TCP to slightly lower temperatures. Moreover, the transformation tends to be accelerated with increasing Mg content.

Other endothermic peaks are observed at a temperature of about 1290 °C for all powders that can be related to the formation of a eutectic melt between α-$Ca_2P_2O_7$ and $Ca_3(PO_4)_2$. As observed by Destainville et al. [23], this peak can be detected in calcium phosphate powders with more than 0.5 wt.% $Ca_2P_2O_7$, indicating that the β-TCP powders obtained in this work contain $Ca_2P_2O_7$. A $Ca_2P_2O_7$ content of approximately 10 wt.% was calculated from the (Ca + Mg)/P molar ratios given in Table 1. It is possible that this phase, together with the magnesium addition, alters the β → α phase transformation temperature. Ryu et al. [24] observed, that although the presence of $Ca_2P_2O_7$ did not affect the shrinkage rate of β-TCP phase, there was a shift of about 50 °C of the β–α transformation, from 1180 °C of stoichiometric TCP [25] to 1230 °C.

3.3. Sintering

The densification of calcium phosphate powders upon heating was examined by dilatometric measurements in samples without previous calcination. Fig. 7 shows the linear shrinkage of powders with different Mg content. Shrinkage starts at approximately 700 °C for all powders. The total linear shrinkage increases with increasing Mg content from ∼26% to ∼29.5% for 1 and 4.5 Mg powders, respectively. Looking at the linear shrinkage behavior (Fig. 7) at 1000 °C, it can be noticed that 1.5 Mg powder shows a higher linear shrinkage of about 19% compared to 1 Mg with about 13.5%. The higher final linear shrinkage of 4.5 Mg can be explained due to changes in the sintering

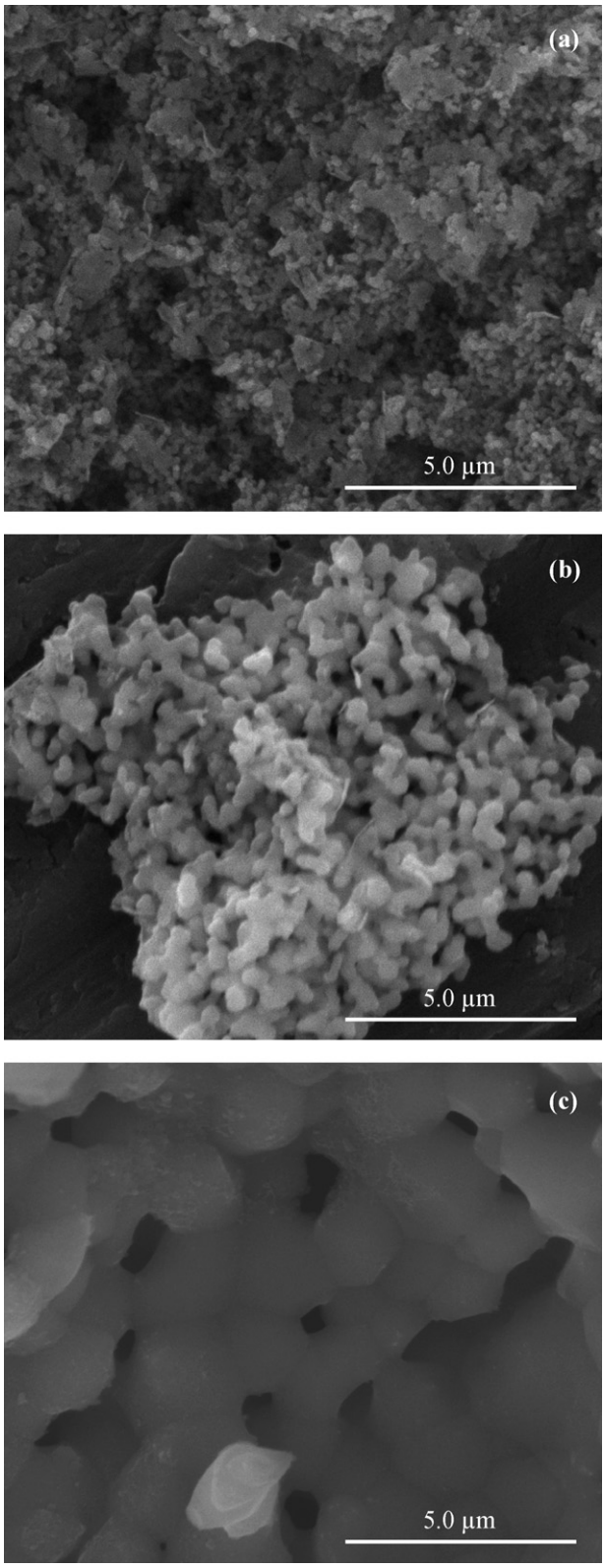

Fig. 5. Scanning electron micrographs of tricalcium phosphate powders with 1.5 mol% Mg substitution after calcination at several temperatures for 3 h: (a) 750 °C; (b) 900 °C; (c) 1050 °C.

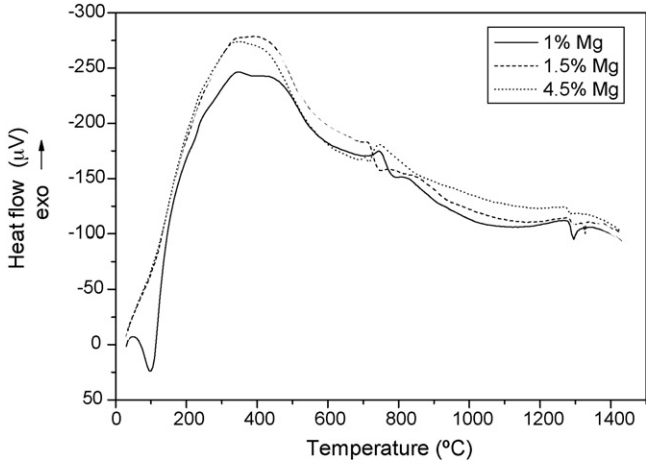

Fig. 6. Differential thermal analysis in air atmosphere of calcium phosphate powders with different amount of Mg substitution.

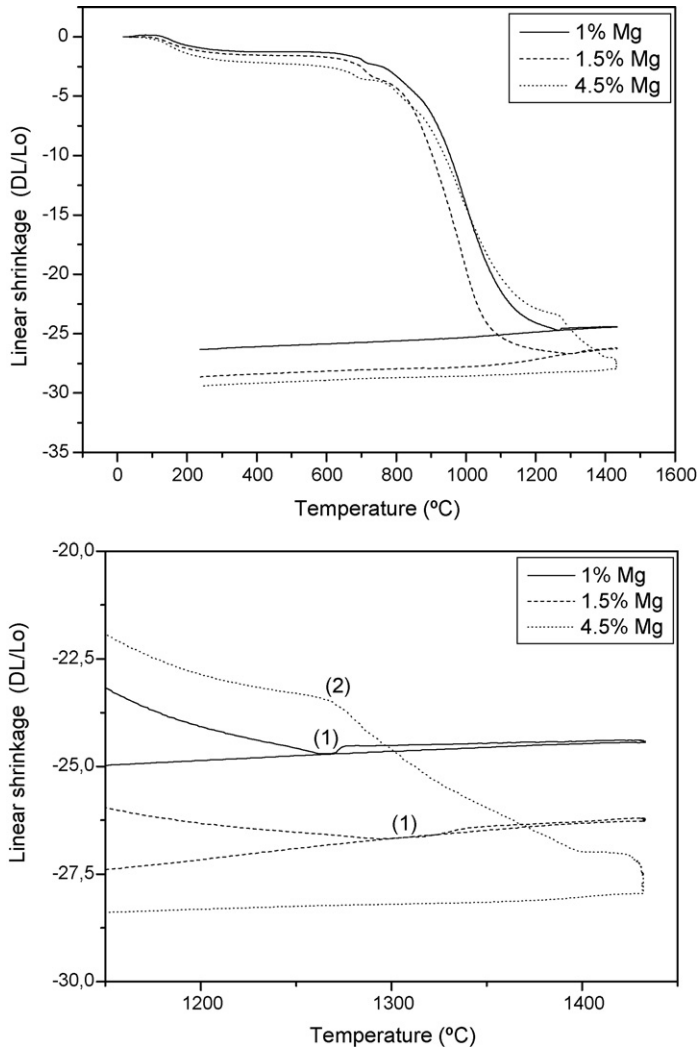

Fig. 7. Linear shrinkage of calcium phosphate powders with different amount of Mg substitution: (1) temperature of β to α phase transformation and (2) acceleration in sintering process.

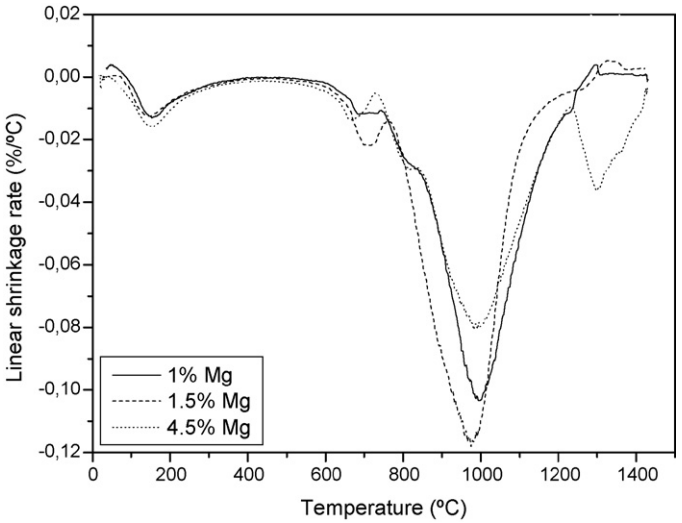

Fig. 8. Linear shrinkage rate of calcium phosphate powders with different amount of Mg substitution.

mechanisms for these powders, as indicated by a change in the linear shrinkage slope that occurs at about 1270 °C, which corresponds to an acceleration in the sintering process. Up to 1400 °C a higher linear shrinkage is observed for this powder, and no β–α TCP phase transformation occurs.

Fig. 8 shows the linear shrinkage rate of powders with different Mg amount, where four peaks can be observed. As the powders were not previously calcinated, the first peak, at about 160 °C, is related to the water loss in the structure of all powders. The alteration in linear shrinkage rate due to the phase transformation of CDHA into β-TCP is characterized by the presence of peaks observed at 650–800 °C, which are in good agreement with differential thermal analysis. The maximum of shrinkage rates occurs in the same temperature interval at about 1000 °C. The temperatures where shrinkage is terminated correspond well with the β–α phase transition temperatures, as observed by expansion at about 1270 and 1330 °C, respectively for 1 and 1.5 Mg powders (Fig. 8). This behavior fits well with X-ray diffraction results, which indicates that the β–α TCP phase transformation occurs at about this temperature for the 1 Mg sample, once at 1300 °C both β-TCP and α-TCP phases were identified.

The β–α transformation can be determined considering a slight linear expansion due to the lower density of the α-TCP phase compared to the β-TCP phase, and, consequently, an increase in lattice volume. At the temperature of β–α phase transformation, there is a blockage in the sintering process and at higher temperatures, no shrinkage is observed. Due to the β-stabilization by substitution of Ca by Mg, with a consequent incorporation of the smaller Mg^{2+} ions on Ca(V) sites in the TCP lattice [14], higher sintering temperatures are possible with increasing Mg content, resulting in a higher total shrinkage.

It is well known that the phase formation in general hinders the densification process, as indicated by a minimum peak in linear shrinkage rate. Once the new phase has completely been formed, densification proceeds again. Considering samples with lower Mg amounts (up to 1.5), the expansion observed is due to the β–α phase transformation. Samples with higher Mg amount (4.5%) do not show the β–α transformation, which might indicate that the densification process of this calcium phosphate composition is associated with a liquid phase formation.

4. Conclusions

Mg-substituted tricalcium phosphate ceramics were obtained from an aqueous solution of calcium hydroxide, orthophosphoric acid and magnesium oxide, after calcination at elevated temperatures.

The presence of magnesium substituted in the β-TCP lattice alters the transformation from CDHA to TCP to slightly lower temperatures and increases the β–α transformation temperature. Incorporation of magnesium into the TCP lattice increases the specific surface area of wet chemically synthesized powders and, consequently, accelerates the sintering process.

The results show that the addition of small amounts of Mg (up to 1.5 mol%) are adequate to postpone the β–α TCP phase transformation to 1330 °C and to accelerate the densification process during sintering of β-TCP ceramics.

Acknowledgements

The authors would like to thank DAAD (Deutscher Akademischer Austausch Dienst) and CAPES (Coordenação de Aperfeiçoamento de Pessoal de Nível Superior, Brasil) for financial support within the frame of PROBRAL project 138-02.

References

[1] L.L. Hench, J. Wilson, An Introduction to Bioceramics. Adv. Series in Ceramics, vol. 1, World Scientific, USA, 1998.
[2] R.Z. Legeros, Calcium Phosphates in Oral Biology and Medicine, in: H.M. Myers (Ed.), Monographs in Oral Science, vol. 15, Karger, 1991.
[3] J.C. Elliot, Structure and Chemistry of the Apatites and Other Calcium Orthophosphates, Studies in Inorganic Chemistry, vol. 18, Elsevier Science BV, 1994.
[4] M. Yashima, A. Sakai, Chem. Phys. Lett. 372 (2003) 779–783.
[5] K.T. Sugiyama, Phys. Chem. Miner. 15 (1987) 125–130.
[6] S.N. Radin, P. Ducheyne, J. Biomed. Mater. Res. 27 (1993) 35–44.
[7] R. Famery, N. Richard, P. Boch, Ceram. Int. 20 (1994) 327–336.
[8] J. Pan, J. Huang, C.Y. Shao, J. Mater. Sci. 38 (2003) 1049–1056.
[9] S. Raynaud, E. Champion, D. Bernache-Assollant, P. Thomas, Biomaterials 23 (2002) 1065–1072.
[10] S.R. Kim, J.H. Lee, Y.T. Kim, D.H. Riu, S.J. Jung, Y.J. Lee, S.C. Chung, Y.H. Kim, Biomaterials 24 (2003) 1389–1398.
[11] I. Mayer, R. Schlam, F.D.B. Featherstone, J. Inorg. Biochem. 1 (1997) 1–6.
[12] A. Bigi, G. Cojazzi, S. Panzavolta, A. Ripamonti, N. Roveri, M. Romanello, K.N. Suarez, L. Moro, J. Inorg. Biochem. 68 (1997) 45–51.
[13] T.J. Webster, C. Ergun, R.H. Doremus, R. Bizios, J. Biomed. Mater. Res. 59 (2002) 312–317.
[14] R. Enderle, F.G. Neunhoeffer, M. Gobbels, F.A. Muller, P. Greil, Biomaterials 26 (2005) 3379–3384.
[15] K. Itatani, M. Takahashi, F.S. Howell, M. Aizawa, J. Mater. Sci.: Mater. Med. 13 (2002) 707–713.
[16] J.D.B. Feathestone, I. Mayer, F.C.M. Driessens, R.M.H. Verbeeck, H.J.M. Heijligers, Inorg. Chim. Acta 80 (1983) 19–23.
[17] R.N. Correia, M.C.F. Magalhaes, P.A.A.P. Marques, A.M.R. Senos, J. Mater. Sci.: Mater. Med. 7 (1996) 501–505.
[18] A. Yasukawa, S. Ouchi, K. Kandori, T. Ishikawa, J. Mater. Chem. 6 (1996) 1401.
[19] I. Mayer, R. Schlam, J.D.B. Featherstone, J. Inorg. Biochem. 66 (1997) 1–6.
[20] I.R. Gibson, W. Bonfield, J. Mater. Sci.: Mater. Med. 13 (2002) 685–693.
[21] H.S. Ryu, K.S. Hong, J.K. Lee, D.J. Kim, J.H. Lee, B.S. Hang, D. Lee, C.K. Lee, S.S. Chung, Biomaterials 25 (2004) 393–401.
[22] C. Ergun, T.J. Webster, R. Bizios, R.H. Doremus, J. Biomed. Mater. Res. 59 (2002) 305–311.
[23] A. Destainville, E. Champion, D. Bernache-assollant, E. Laborde, Mater. Chem. Phys. 80 (2003) 269–277.
[24] H.S. Ryu, H.J. Youn, K.S. Hong, B.S. Chang, C.K. Lee, S.S. Chung, Biomaterials 23 (2002) 909–914.
[25] G. Tromel, Stahl u. Eisen 63 (1943) 21.